International Journal of Solids and Structures 51 (2014) 1246–1252

Contents lists available at ScienceDirect

International Journal of Solids and Structures

journal homepage: www.elsevier.com/locate/ijsolstr

Free-edge interlaminar stress analysis of piezo-bonded composite laminates under symmetric electric excitation

Bin Huang, Heung Soo Kim *

Department of Mechanical, Robotics and Energy Engineering, Dongguk University-Seoul, 30 Pildong-ro, 1-gil, Jung-gu, Seoul 100-715, Republic of Korea

ARTICLE INFO

Article history:
Received 14 August 2013
Received in revised form 3 December 2013
Available online 15 December 2013

Keywords:
Interlaminar stress
Free-edge
Laminated composite
Piezo
Stress function

ABSTRACT

A stress function-based approach is proposed to analyze the free-edge interlaminar stresses of piezo-bonded symmetric laminates. The proposed method satisfies the traction free boundary conditions, as well as surface free conditions. The symmetric laminated structure was excited under electric fields that can generate induced strain, resulting in pure extension in the laminated plate. The governing equations were obtained by taking the principle of complementary virtual work. To verify the proposed method, cross-ply, angle-ply and quasi-isotropic laminates were analyzed. The stress concentrations predicted by the present method were compared with those analyzed by the finite element method. The results show that the stress function-based analysis of piezo-bonded laminated composite structures is an efficient and accurate method for the initial design stage of piezo-bonded composite structures.

1. Introduction

Recently, piezoelectric actuators and sensors are most commonly used in smart structures, modern control engineering and energy harvesting industries, because of their large electromechanical coupling effect, wide bandwidth and quick response (Kapuria et al., 2010; Kim et al., 2011). Fiber reinforced laminated composite materials have many advantages, compared with other metal and nonmetal materials in physics (Herakovich, 2012). These composite materials could be good candidates for enhancement, to replace the substrate materials of smart structures. The development of piezo-bonded composite laminates with their mathematical modeling provides many engineering applications (Chopra, 2002). These smart structures could be applied in many advanced engineering fields, such as aircraft structures, satellites, large space structures, and auto-motives. However, delamination is one of the major failure mechanisms in piezo-bonded composite laminates, due to interlaminar stresses at layer interfaces.

Since the last several decades, three-dimensional interlaminar stress and stress singularity study of these structures have received considerable attention (Pipes and Pagano, 1970; Rhee et al., 2006; Kim et al., 2008, 2010; Izadi and Tahani, 2010; Lee et al., 2011; Kassapoglou and Lagace, 1986). A large volume of literature achievements has been established from experimental, as well as theoretical investigations. The presence of material and geometric discontinuities resulted in stress concentrations at the free edges, which is also referred to as free edge effects or boundary layer effects (Wang and Choi, 1982a,b). Free-edge effects are critical to interlaminar failure or delamination of piezo and composite layers. Due to the piezoelectric coupling effects in piezo-bonded composite laminates, the free edge effects become more complicated. Analysis of these localized interlaminar stresses at the free edge is of great importance in the initial design of piezoelectric composite laminates.

There are various theories (Ghugal and Shimpi, 2002), based on displacement fields or stress fields, for predicting the flexural response of laminated plates with surface-bonded or embedded induced strain actuators. Among the displacement fields-based theories, classical lamination theory (CLT) (Lee, 1990; Konieczny and Woźniak, 1994; Wang et al., 1997), three equivalent single-layer shear deformation theories (ESLSDT) (Kabir, 1996; Reddy, 1999), layerwise shear deformation theory (LWSDT) Robbins and Reddy, 1993; Zhu and Lam, 1998; Kim et al., 2002a,b; Kim et al., 2006) and finite element methods (Chandrashekhara and Agarwal, 1993; Detwiler et al., 1995) are the most popularly used theories. However, CLT shows great inadequacy for the stress analysis of piezo-bonded composite laminates, as CLT assumes a linear displacement distribution across the thickness of entire laminates, and neglects the transverse shear deformation, which is necessary for moderately thick and thick laminates. ESLSDT cannot recover transverse shear stress continuity in the thickness direction by using the constitutive relations, which are discontinuous at interfaces between layers, and are against equilibrium conditions. LWSDT are the most accurate in displacement fields-based theories, but they are more computationally inefficient than

* Corresponding author. Tel.: +82 2 2260 8577; fax: +82 2 2263 9379.
E-mail address: heungsoo@dgu.edu (H.S. Kim).

0020-7683/$ - see front matter © 2013 Elsevier Ltd. All rights reserved.
http://dx.doi.org/10.1016/j.ijsolstr.2013.12.016

ESLSDT, due to their demand for a large number of unknown variables.

Another approach to analyze laminated composite structure is stress function-based theory, which can fully satisfy not only stress continuity, but also traction free boundary conditions. These theories have great potential in the future study of interlaminar stress analysis of piezo-bonded composite laminates. After Spilker and Chou (1980) demonstrated the importance of satisfying the traction free boundary conditions at the free edges, Yin (1994a,b) proposed a variational method, using piecewise polynomial approximations based on stress-based layerwise theory (SBLWT). The stress functions involved in his approach not only satisfy pointwise equilibrium equation, but also continuity of interlaminar stress over each layer, and at the layer interfaces. Flanagan (1994) proposed a solution method based on a series expansion of mode shapes of a clamped–clamped beam, for determining the free-edge stresses in composite laminates. His approach can be concluded in stress-based equivalent single-layer theory (SBESLT) that is computationally more efficient than Yin's work. While Flanagan's method can well predict the interlaminar stresses along the in-plane direction, the interlaminar stresses along the thickness direction show oscillations. Flanagan's work was improved by Cho and Kim (2000) and Kim et al. (2000), by using an extended Kantorovich method. In their works, converged stress distributions obtained under extension, bending, twisting and thermal loading are independent of the number of initially assumed stress functions, and the oscillations appearing in the thickness direction can be reduced, or even eliminated.

Actuating force of piezoelectric layer causes stress concentration at the free edge of smart composite laminates. The concentrated stress could initiate debonding of the actuator and lead failure of the smart composite laminates. However, most researches have been focused on global responses of the smart composite laminates such as vibration control, energy harvesting and structural health monitoring and so on (Chopra, 2002; Kim et al., 2011). Kapuria and Kumari focused on stress concentration of piezolaminated panels under electromechanical coupling load (Kapuria and Kumari, 2013). They provided accurate three dimensional piezoelasticity solutions using extended Reissner-type variational principle and extended Kantorovich method. In this work, we will investigate stress concentration of piezo-bonded smart composite laminates under piezoelectric excitation using stress variables only. The principle of complementary virtual work is adopted to derive governing equations. Various layup configurations are studied, to verify the proposed approach. The proposed method is also evaluated by comparing finite element analysis results, using the commercially available package ANSYS.

2. Formulations

Fig 1 shows a symmetric configuration of piezo-bonded composite laminates with free edges. Two piezoelectric actuators are bonded on the top and bottom surfaces of the laminated composites. The composite laminates consist of orthotropic materials, and have arbitrary fiber angles with respect to the x axis. The thicknesses of piezoelectric actuators and composite laminates are considered the same in each layer, for convenience. This structure can be extended, bended, and twisted under electric excitation, due to the electro-mechanical coupling of the piezoelectric actuators.

Based on the linear elasticity, the general form of the constitutive equations can be expressed for each layer in Eq. (1). Induced strains ($[d][E]$) only exist in piezoelectric layers. A piezoelectric strain matrix $[d]$ is defined at each layer, and it has zero values for composite layers. Pure extension by the piezoelectric excitation is considered in the present study. Therefore, electric fields $\{E\}$ are applied through the thickness direction only, and E_1 and E_2 are zero.

$$\begin{Bmatrix}\varepsilon_1\\ \varepsilon_2\\ \varepsilon_3\\ \varepsilon_4\\ \varepsilon_5\\ \varepsilon_6\end{Bmatrix} = \begin{bmatrix} S_{11} & S_{12} & S_{13} & 0 & 0 & S_{16}\\ S_{21} & S_{22} & S_{23} & 0 & 0 & S_{26}\\ S_{31} & S_{32} & S_{33} & 0 & 0 & S_{36}\\ 0 & 0 & 0 & S_{44} & S_{45} & 0\\ 0 & 0 & 0 & S_{54} & S_{55} & 0\\ S_{61} & S_{62} & S_{63} & 0 & 0 & S_{66}\end{bmatrix}\begin{Bmatrix}\sigma_1\\ \sigma_2\\ \sigma_3\\ \sigma_4\\ \sigma_5\\ \sigma_6\end{Bmatrix} + \begin{bmatrix} 0 & 0 & d_{31}\\ 0 & 0 & d_{32}\\ 0 & 0 & d_{33}\\ 0 & d_{24} & 0\\ d_{15} & 0 & 0\\ 0 & 0 & 0\end{bmatrix}\begin{Bmatrix}E_1\\ E_2\\ E_3\end{Bmatrix} \tag{1}$$

The first row of Eq. (1) can be rewritten into the following form.

$$\sigma_1 = \frac{\varepsilon_1 - S_{1j}\sigma_j - d_{31}E_3}{S_{11}}, \quad (j = 2,3,\ldots,6) \tag{2}$$

Substituting Eq. (2) into Eq. (1), all other strains can then be expressed as follows.

$$\varepsilon_i = \hat{S}_{ij}\sigma_j + \frac{S_{i1}}{S_{11}}\varepsilon_1 + \hat{d}_{3i}E_3, \quad (i,\ j = 2,3,\ldots,6) \tag{3}$$

where,

$$\hat{S}_{ij} = S_{ij} - \frac{S_{i1}S_{1j}}{S_{11}}, \quad \hat{d}_{3i} = d_{3i} - \frac{S_{i1}}{S_{11}}d_{31} \tag{4}$$

The boundary conditions for the given geometric configuration at the free edges, and at the top and bottom surfaces, are given in the following equations.

$$\begin{aligned}&\sigma_2 = \sigma_4 = \sigma_6 = 0 \quad \text{at } y = 0, b\\ &\sigma_3 = \sigma_4 = \sigma_5 = 0 \quad \text{at } z = \pm H/2\end{aligned} \tag{5}$$

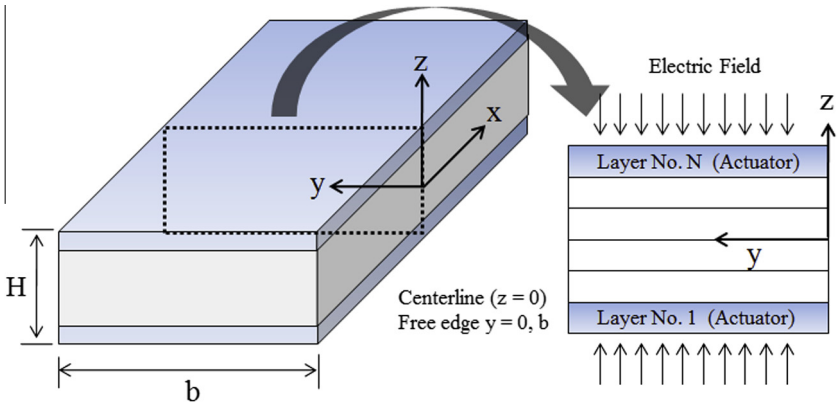

Fig. 1. Geometry of piezo-bonded composite laminate.

The smart composite laminate is considered long enough. Then, generalized plane strain states could be assumed, and the stress fields are independent of the x-axis. The non-dimensional coordinates are introduced as follows.

$$\eta = z/h \qquad \xi = y/h \tag{6}$$

Lekhnitskii stress functions (Lekhnitskii, 1963) are introduced to satisfy the pointwise equilibrium equations automatically. These stress functions can be divided into in-plane, and out-of-plane functions.

$$\sigma_2 = \frac{\partial^2 F}{\partial \eta^2}, \quad \sigma_3 = \frac{\partial^2 F}{\partial \xi^2}, \quad \sigma_4 = -\frac{\partial^2 F}{\partial \xi \partial \eta} \qquad \sigma_5 = -\frac{\partial \psi}{\partial \xi}, \quad \sigma_6 = \frac{\partial \psi}{\partial \eta} \tag{7}$$

where,

$$F = \sum_{i=1}^{n} f_i(\xi) g_i(\eta), \quad \psi = \sum_{i=1}^{n} p_i(\xi) g_i^I(\eta) \tag{8}$$

The superscript I in Eq. (8) denotes differentiation of the function with respect to η. The out-of-plane functions $g_i(\eta)$ must satisfy the traction free boundary conditions at the top and bottom surfaces (i.e. the stress functions and their first derivatives should be zero in those places). The out-of plane functions are assumed to be the mode shape functions of a clamped–clamped beam. Since solutions are sensitive to initially assumed stress functions and odd function set causes singularity in the eigenvalue solution procedure for the given symmetric configuration, an even function set of a clamped–clamped beam is used for the extension problem. The out-of-plane stress functions $g_i(\eta)$ are given as follows, and are presented in Fig. 2.

$$g_i(\eta) = \cos(\beta_i \eta) + k_i \cos h(\beta_i \eta) \tag{9}$$

where,

$$k_i = \cos(\beta_i/2) \sec h(\beta_i/2) \tag{10}$$

The coefficients β_i are the solutions of the following characteristic equation.

$$\cos h(\beta/2) \sin(\beta/2) + \cos(\beta/2) \sin h(\beta/2) = 0 \tag{11}$$

The governing equations are obtained by taking the principle of complementary virtual work. The complementary strain energy is calculated by

$$\partial U = \int \int \varepsilon_i \sigma_i dy dz = 0 \tag{12}$$

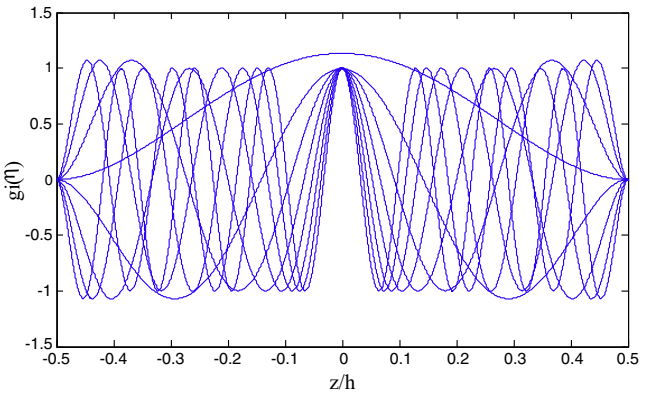

Fig. 2. Initially assumed out-of-plane stress functions $g_i(\eta)$.

Substituting Eqs. (3) and (7) into Eq. (12), the complementary strain energy can be rewritten as follows.

$$\partial U = \int \int \left[\sigma_j \hat{S}_{ij} \sigma_i + \left(\frac{S_{i1}}{S_{11}} \varepsilon_1 + \hat{d}_{3i} E_3 \right) \sigma_i \right] d\xi d\eta = 0 \quad (i, j = 2, 3, \ldots, 6) \tag{13}$$

Eq. (13) is reduced to the following form after integration by parts, and applying the boundary conditions at the free edge.

$$\int \left[a_{ij}^{(4)} f_{j,\xi\xi\xi\xi} + a_{ij}^{(2)} f_{j,\xi\xi} + a_{ij}^{(0)} f_j + b_{ij}^{(2)} p_{j,\xi\xi} + b_{ij}^{(0)} p_j + r_i \right] \delta f_i d\xi + \int \left[d_{ij}^{(2)} f_{j,\xi\xi} + d_{ij}^{(0)} f_j + c_{ij}^{(2)} p_{j,\xi\xi} + c_{ij}^{(0)} p_j + s_i \right] \delta p_i d\xi = 0, \quad (i, j = 1, 2, \ldots, n) \tag{14}$$

where,

$$\begin{aligned}
a_{ij}^{(4)} &= \int \hat{S}_{33} g_i g_j d\eta \\
a_{ij}^{(2)} &= \int \hat{S}_{23} (g_i^{II} g_j + g_i g_j^{II}) d\eta - \int \hat{S}_{44} g_i^I g_j^I d\eta \\
a_{ij}^{(0)} &= \int \hat{S}_{22} g_i^{II} g_j^{II} d\eta \\
b_{ij}^{(2)} &= \int \hat{S}_{36} g_i g_j^{II} d\eta - \int \hat{S}_{45} g_i^I g_j^I d\eta \quad b_{ij}^{(0)} = \int \hat{S}_{26} g_i^{II} g_j^{II} d\eta \\
d_{ij}^{(2)} &= \int \hat{S}_{36} g_i^{II} g_j d\eta - \int \hat{S}_{45} g_i^I g_j^I d\eta \quad d_{ij}^{(0)} = \int \hat{S}_{26} g_i^{II} g_j^{II} d\eta \\
c_{ij}^{(2)} &= -\int \hat{S}_{55} g_i^I g_j^I d\eta \quad c_{ij}^{(0)} = \int \hat{S}_{66} g_i^{II} g_j^{II} d\eta \\
r_i &= \int \left(\frac{S_{21}}{S_{11}} \varepsilon_1 + \hat{d}_{32} E_3 \right) g_i^{II} d\eta \quad s_i = \int \left(\frac{S_{61}}{S_{11}} \varepsilon_1 + \hat{d}_{36} E_3 \right) g_i^{II} d\eta
\end{aligned} \tag{15}$$

In Eq. (14), the governing equations reduce to the 2nd and 4th order ordinary differential equations, where $f_i(\xi)$ and $p_i(\xi)$ are coupled. The homogeneous solutions of f_i and p_i are assumed to be of the following form.

$$f_i^{(H)} = v_i^f e^{\lambda \xi}, \quad p_i^{(H)} = v_i^p e^{\lambda \xi} \tag{16}$$

Substituting Eq. (16) into Eq. (14), the 2nd and 4th order coupled ordinary differential equations are reduced to the following eigenvalue problem.

$$\begin{aligned}
&a_{ij}^{(0)} v_j^f + (a_{ij}^{(2)} + \lambda^2 a_{ij}^{(4)}) \lambda^2 v_j^f + (\lambda^2 b_{ij}^{(2)} + b_{ij}^{(0)}) v_j^p = 0 \\
&d_{ij}^{(0)} v_j^f + d_{ij}^{(2)} \lambda^2 v_j^f + (c_{ij}^{(0)} + \lambda^2 c_{ij}^{(2)}) v_j^p = 0, \quad (i, j = 1, 2, 3, \ldots, n) \\
&\lambda^2 v_j^f - v_j^{fII} = 0, \quad (i, j = 1, 2, \ldots, 6)
\end{aligned} \tag{17}$$

The 3rd equation of Eq. (17) is an auxiliary equation for conversion to a standard form of a generalized eigenvalue problem, as follows.

$$\begin{bmatrix} a_{ij}^{(0)} & a_{ij}^{(2)} & b_{ij}^{(0)} \\ d_{ij}^{(0)} & d_{ij}^{(2)} & b_{ij}^{(0)} \\ 0 & -I & 0 \end{bmatrix} \begin{bmatrix} v_j^f \\ v_j^{fII} \\ v_j^p \end{bmatrix} = \lambda^2 \begin{bmatrix} 0 & -a_{ij}^{(4)} & -b_{ij}^{(2)} \\ 0 & 0 & c_{ij}^{(0)} \\ -I & 0 & 0 \end{bmatrix} \begin{bmatrix} v_j^f \\ v_j^{fII} \\ v_j^p \end{bmatrix}, \quad (i, j = 1, 2, \ldots, n) \tag{18}$$

Since the interlaminar stresses decay in the interior region of the laminates, only negative roots of λ^2 are selected in Eq. (18). From the eigenvalue problem, $3n$ eigenvalues are obtained, and the homogeneous solutions are obtained by a $3n$-terms linear combination.

$$\begin{aligned}
f_i^{(H)} &= t_j v_{ij}^f e^{-\lambda_j \xi} \\
p_i^{(H)} &= t_j v_{ij}^p e^{-\lambda_j \xi}, \quad (i = 1, 2, \ldots, n), \quad (j = 1, 2, \ldots, 3n)
\end{aligned} \tag{19}$$

where t_j are constants to be determined from the boundary conditions.

The particular solution can be obtained from the assumption that $f_i(\xi)$ and $p_i(\xi)$ are constants in Eq. (14), so that all their derivatives are zero. The remaining parts of Eq. (14) reduce to the following equations.

$$\begin{aligned} &a_{ij}^{(0)} f_j^{(\mathrm{P})} + b_{ij}^{(0)} p_j^{(\mathrm{P})} = -r_i \\ &b_{ij}^{(0)} f_j^{(\mathrm{P})} + c_{ij}^{(0)} p_j^{(\mathrm{P})} = -s_i, \quad (i,j = 1,2,\ldots,n) \end{aligned} \tag{20}$$

After solving the particular solutions, the in-plane stress functions can be obtained, and expressed as the summation of the homogeneous solution and particular solution.

$$\begin{aligned} &f_i = f_i^{(\mathrm{H})} + f_i^{(\mathrm{P})} \\ &p_i = p_i^{(\mathrm{H})} + p_i^{(\mathrm{P})}, \quad (i = 1,2,\ldots,n) \end{aligned} \tag{21}$$

Finally, the constants t_j are determined from the traction free boundary conditions of σ_2, σ_4 and σ_6 at the free edge, as shown in Eq. (5).

$$\begin{aligned} &t_j v_{ij}^f + f_i^{(\mathrm{P})} = 0 \\ &t_j v_{ij}^f = 0 \\ &t_j v_{ij}^p + p_i^{(\mathrm{P})} = 0, \quad (i = 1,2,\ldots,n), \quad (j = 1,2,\ldots,3n) \end{aligned} \tag{22}$$

Substituting the calculated in-plane stress function into Eq. (7), the interlaminar stresses can be obtained as follows.

$$\begin{aligned} \sigma_2 &= \left(t_j v_{ij}^f e^{-\lambda_j \xi} + f_i^{(\mathrm{P})}\right) \mathrm{g}_i^{\mathrm{II}} \\ \sigma_3 &= \lambda_i^2 t_j v_{ij}^f e^{-\lambda_j \xi} \mathrm{g}_i \\ \sigma_4 &= \lambda_j t_j v_{ij}^f e^{-\lambda_j \xi} \mathrm{g}_i^{\mathrm{I}} \\ \sigma_5 &= \lambda_j t_j v_{ij}^p e^{-\lambda_j \xi} \mathrm{g}_i^{\mathrm{I}} \\ \sigma_6 &= \left(t_j v_{ij}^p e^{-\lambda_j \xi} + p_i^{(\mathrm{P})}\right) \mathrm{g}_i^{\mathrm{II}}, \quad (i = 1,2,\ldots,n), \quad (j = 1,2,\ldots,3n) \end{aligned} \tag{23}$$

The classical lamination theory, which is based on the plane stress assumption, is also investigated for piezo-bonded composite laminates, in order to compare with the proposed stress function based approach. The reduced constitutive relationships for each ply are shown in the following form (Chattopadhyay and Seeley, 1997).

$$\begin{bmatrix} \sigma_1 \\ \sigma_2 \\ \sigma_6 \end{bmatrix}_k = \begin{bmatrix} \bar{Q}_{11} & \bar{Q}_{12} & \bar{Q}_{16} \\ \bar{Q}_{12} & \bar{Q}_{22} & \bar{Q}_{26} \\ \bar{Q}_{16} & \bar{Q}_{26} & \bar{Q}_{66} \end{bmatrix}_k \begin{bmatrix} \varepsilon_1^0 - \Lambda_1 \\ \varepsilon_2^0 - \Lambda_2 \\ \varepsilon_6^0 \end{bmatrix}_k \tag{24}$$

where, Λ_1 and Λ_2 represent the induced strain by piezoelectric actuators, and ε_i^0 represents the mid plane strain. Although the strains are continuous throughout the thickness, in-plane stresses are not necessarily continuous, due to different elastic properties for each ply.

3. Numerical results

To verify the proposed approach, cross-ply, angle-ply and quasi-isotropic laminates are considered in the present study. The material properties of composite laminates are given as follows (Tahani and Nosier, 2003)

$$\begin{aligned} &E_1 = 138\ \text{Gpa}, \quad E_2 = E_3 = 14.5\ \text{Gpa} \\ &G_{12} = G_{13} = G_{23} = 5.9\ \text{Gpa} \\ &v_{12} = v_{31} = v_{23} = 0.21 \end{aligned} \tag{25}$$

The PZT-5H is used as a piezoelectric actuator, and its material properties are given as follows (Chopra, 2002)

$$\begin{aligned} &E_1 = E_2 = 61\ \text{Gpa}, \quad E_3 = 48\ \text{Gpa} \\ &G_{12} = 23.5\ \text{Gpa}, \quad G_{13} = G_{23} = 5.9\ \text{Gpa} \\ &v_{12} = v_{31} = v_{23} = 0.29 \\ &d_{13} = d_{23} = -274 \times 10^{-12}\ \text{m/N}, \quad d_{33} = 593 \times 10^{-12}\ \text{m/N} \end{aligned} \tag{26}$$

The in-plane length 'b' is assumed to be '$4H$', where H is the total thickness of the structure. The lamina thickness is 0.125 mm, which is almost one fourth of the PZT's thickness (0.5 mm). For convenience, 4 laminae, which have the same fiber orientations, are considered as one lamina, so that each lamina thickness is then the same as the PZT's thickness. The in-plane and out-of-plane stress distributions are obtained, and they are compared with three-dimensional finite element analysis results. The three-dimensional finite element analysis results are obtained by the commercial finite element package ANSYS. The Solid 64 element is used for composite laminates, and Solid 5 for PZTs, with a total of 640,281 degrees of freedom. The three-dimensional solid laminate has a relatively long length, compared with the width and height, where the length $L = 40H = 10b$, to express the generalized plane strain state effectively. The clamped-free boundary condition is applied to the x-plane of the laminate. The results are extracted at the inner part of the laminate, where all the boundary layer effects occurring along the x-axis have decayed.

3.1. Convergence study

In the proposed stress function-based approach, the number of initially assumed out-of-plane functions influences the final stress distributions. The stresses are going to converge as the number of initially assumed functions increases. The number of initially assumed functions is defined as a term, and a proper choice of the term is the main task for the convergence problem.

Interlaminar normal stress (σ_3) distribution at the free edge of [PZT/0/90]s laminate under electric excitation is shown in Fig. 3, by using a different number of terms. Because of the assumption of using harmonic functions as out-of-plane stress functions, the present results show some oscillations for out-of-plane stresses. The 8-terms' result shows large oscillation; and with the increase of term number, the oscillations can be reduced dramatically, but small oscillation still exists. The proposed method can also predict the position of maximum stress concentration accurately, which is the interface of the PZT and 0 degree layers. From the figure, the

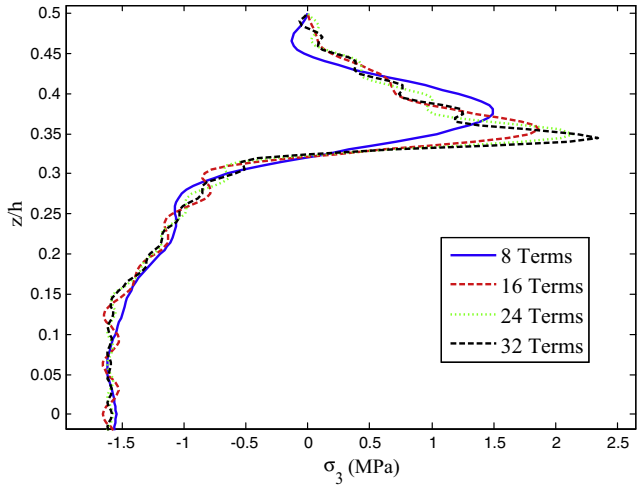

Fig. 3. Interlaminar normal stress (σ_3) distribution at the free edge of [PZT/0/90]s laminate under electric excitation.

concentrated maximum stress approaches the interface of the PZT and 0 degree layers, as the number of terms increases.

The relative errors of peak values for σ_3 are calculated by using the following equation, and are presented in Fig. 4.

$$error(k) = \frac{peak(\sigma_3(k)) - peak(\sigma_3(30))}{peak(\sigma_3(4)) - peak(\sigma_3(30))} \times 100 \quad (27)$$

where $k = 4, 5, \ldots, 29, 30$, represents term numbers. The relative errors are less than 2%, when using 26 terms for σ_3.

Since the 26-term result converges well, numerical results are analyzed by using the 26 initially assumed stress functions. These numerical results can be obtained under the process of MATLAB within 2–3 s, by using a normal dual-core desktop computer.

3.2. Piezoelectric excitation

Numerical results of interlaminar stresses are obtained under piezoelectric excitation, and only the pure extension case is considered in this paper. An electric field of 2×10^5 V/m is applied to both PZTs on the top and bottom surfaces, which can result in pure extension of the whole structure. Results are obtained at the free edge of the laminates, and also at the interface of layers.

Fig 5 shows the interlaminar normal stress (σ_3) and interlaminar shear stress (σ_4) distributions at the PZT/0 interface of [PZT/0/90]s laminate. Interlaminar normal stress is concentrated at the free edge, which may lead to delamination of the PZT layer, and converges to zero in the interior area. The result of three-dimensional finite element method (FEM) also shows the same tendency and magnitude. Interlaminar shear stress satisfies the traction free boundary condition at the free edge, and presents large stress concentration near the free edge. However, FEM result shows a nonzero stress state at the free edge, since the displacement-based theories cannot fully satisfy the traction free boundary condition at the free edge. So, the stress function-based approach shows more accurate results than displacement-based approaches at the free edge. Fig. 6 shows the interlaminar normal and shear stresses distributions at the 0/90 interface of [PZT/0/90]s laminate. The interlaminar normal stress shows a large negative stress concentration at the free edge, which increases the peeling strength at the interface of the 0 and 90 degree layers. The interlaminar normal stress also converges to zero in the interior area. The interlaminar shear stress well matches with the FEM result, and also satisfies the traction free boundary condition exactly.

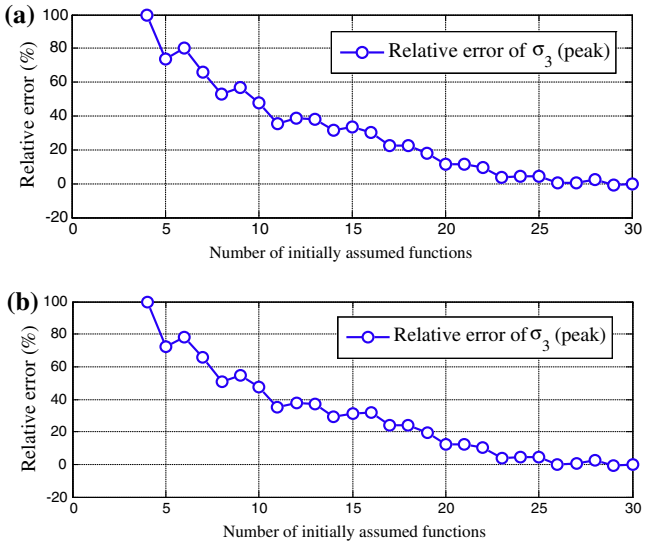

Fig. 4. (a) Relative errors of peak interlaminar stresses [PZT/0/90]s, $n = 4,5,\ldots,29,30$. (b) Relative errors of peak interlaminar stresses [PZT/45/-45]s, $n = 4,5,\ldots,29,30$.

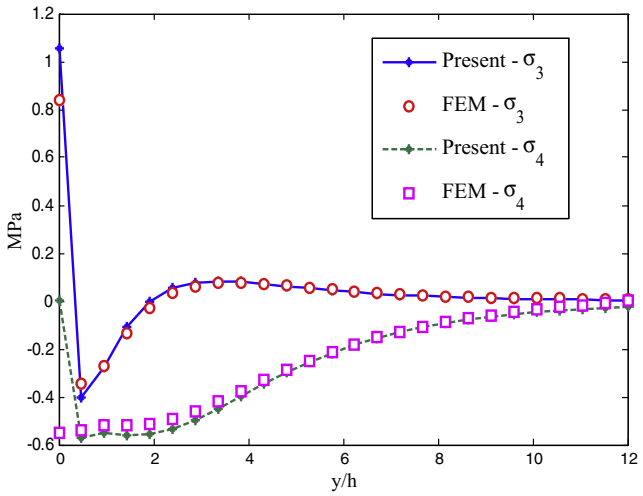

Fig. 5. Interlaminar normal and shear stresses (σ_3 and σ_4) distributions at the PZT/0 interface of [PZT/0/90]s laminate under electric excitation (at $z/h = 1/3$).

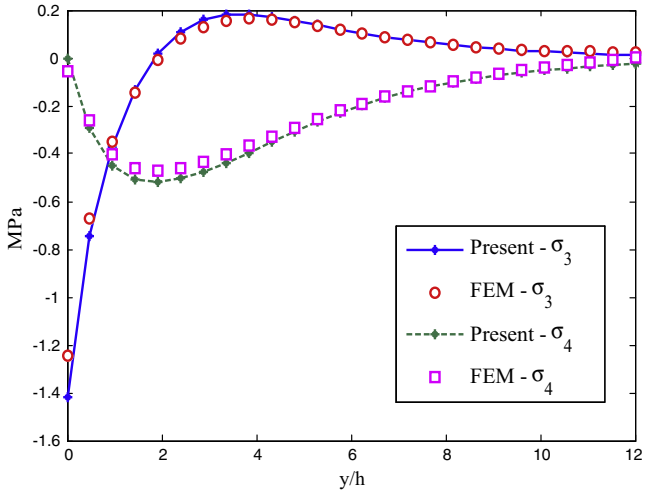

Fig. 6. Interlaminar normal and shear stresses (σ_3 and σ_4) distributions at the 0/90 interface of [PZT/0/90]s laminate under electric excitation (at $z/h = 1/6$).

Fig 7 shows the interlaminar normal and shear stresses (σ_3, σ_4, σ_5) distributions at the PZT/45 interface of the [PZT/45/−45]s laminate. Since the material properties of composite are mainly determined by the fiber orientations, an angle ply ([45/−45]s) generates all interlaminar shear stresses (σ_4, σ_5) near the free edge. Unlike σ_4, σ_5 is concentrated at the free edge, and converges to zero in the interior area. Fig. 8 shows the interlaminar normal and shear stress distributions at the 45/−45 interface of [PZT/45/−45]s laminate. σ_3 and σ_4 have similar stress distributions to [PZT/0/90]s laminate, while this laminate has positive σ_5 across the width direction.

Fig 9 shows the out-of-plane interlaminar normal distribution at the free edge of [PZT/45/−45]s laminate. The proposed approach predicts larger stress concentration at the PZT/45 interface, which represents that finite element analysis, even using fine mesh, could underestimate the stress states of piezo-bonded composite laminates. Even though there is a small difference in the middle layers between the two methods, the proposed result is acceptable, and can be considered as an efficiently refereed result, when compared with other displacement-based approaches. The out-of-plane

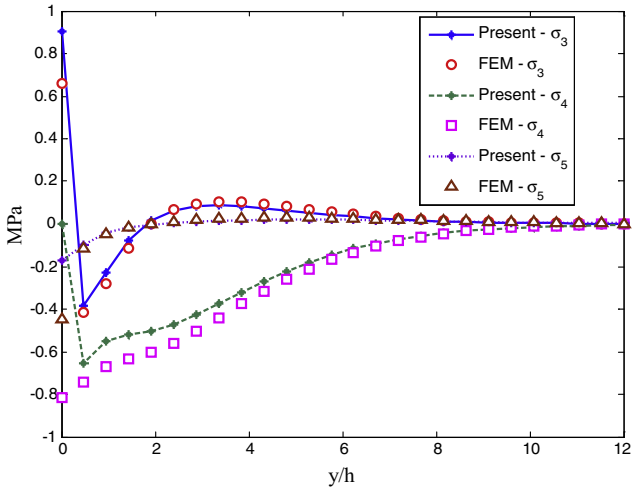

Fig. 7. Interlaminar normal and shear stresses (σ_3, σ_4 and σ_5) distributions at the PZT/45 interface of [PZT/45/-45]s laminate under electric excitation (at $z/h = 1/3$).

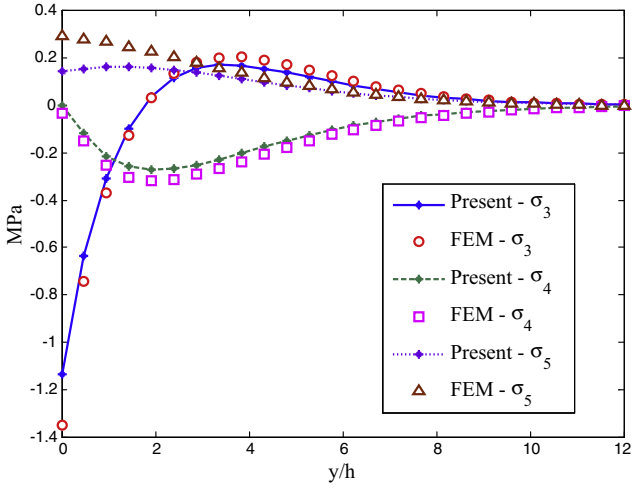

Fig. 8. Interlaminar normal and shear stresses (σ_3, σ_4 and σ_5) distributions at the 45/-45 interface of [PZT/45/-45]s laminate under electric excitation (at $z/h = 1/6$).

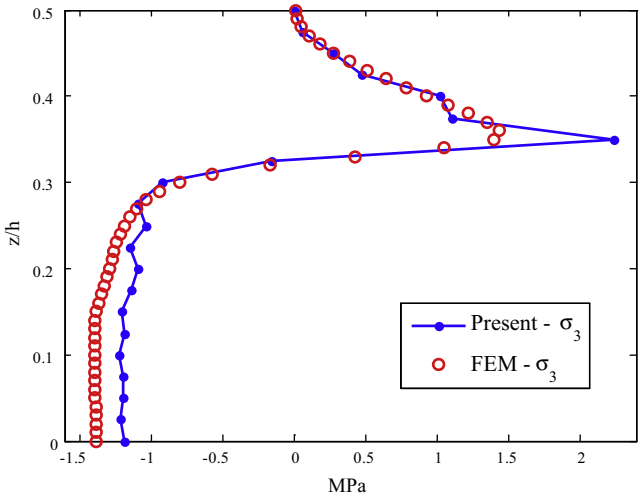

Fig. 9. Interlaminar normal stress (σ_3) distribution at the free edge of [PZT/45/-45]s laminate under electric excitation.

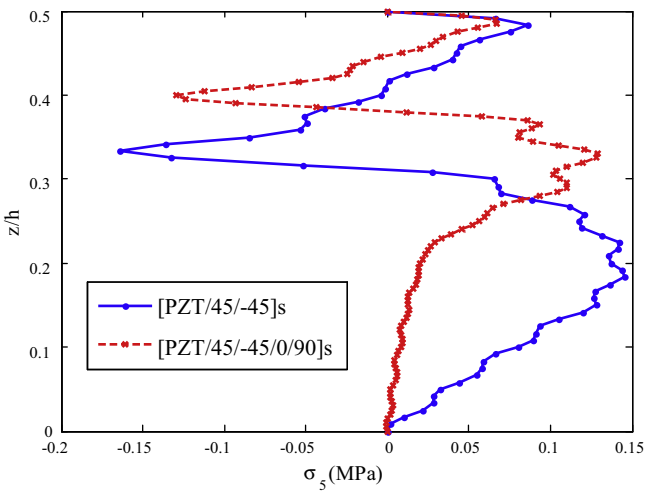

Fig. 10. Interlaminar shear stress (σ_5) distributions at the free edge under electric excitation.

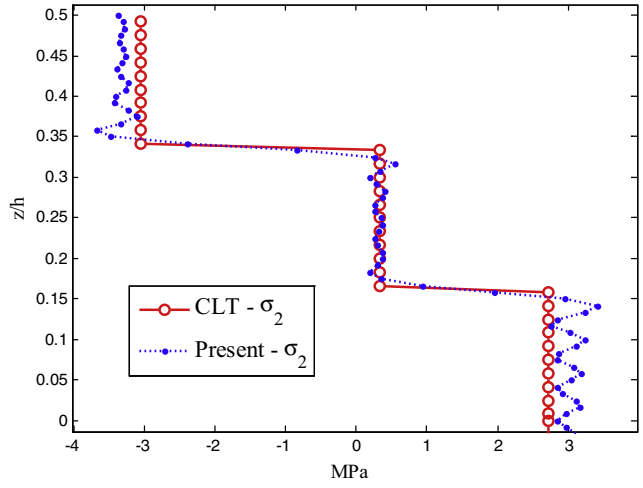

Fig. 11. In-plane normal stress (σ_2) distribution at the interior of [PZT/0/90]s laminate under electric excitation.

interlaminar shear stress (σ_5) distributions for both [PZT/45/-45]s laminate and [PZT/45/-45/0/90]s laminate are shown in Fig. 10. These shear stresses concentrate at PZT interfaces, and satisfy traction free boundary conditions. The magnitude of shear stresses affects the strength of structure.

The CLT solution for in-plane normal stress (σ_2) is obtained in the interior of the laminates, and is compared with the proposed approach in Fig. 11. CLT provides only the interior solution of the laminates, but the proposed method predicts the interior solution accurately, as well as all three-dimensional interlaminar stresses.

4. Conclusions

The interlaminar stresses of piezo-bonded composite laminates have been analyzed by using a stress function-based approach. The proposed method automatically satisfied the pointwise equilibrium equation, as well as traction free boundary conditions. The governing equation was obtained using the complementary virtual work principle. The stress states are analyzed by general eigenvalue solution procedure. Even though small oscillations of inter-

laminar stresses appeared along the thickness direction, they can be reduced, by increasing the number of initially assumed stress functions. The size of the problem depends on the number of initially assumed stress functions, and is independent of the number of stacking layers, which represents that the proposed method is much more efficient than the displacement-based approaches. Large interlaminar stresses were generated and concentrated at the PZT/lamina interface under piezoelectric excitation, which could initiate delamination of the laminates. Delamination decreases the load carrying capability of the laminates. Therefore, accurate stress prediction is an important issue in the design of smart composite laminates. Finite element analysis, even using very fine mesh, underestimated the stress concentration at the PZT/lamina interface, compared to the present method. The proposed method provides an accurate stress state of piezo bonded smart composite laminates. The drawback of the proposed method is that only simple geometry can be analyzed. Therefore, the proposed method can be used as reference data for finite element analysis, or an initial design tool for smart composite structure.

Acknowledgments

This research was supported by the Basic Science Research Program, through the National Research Foundation of Korea (NRF), funded by the Ministry of Education, Science and Technology (NRF-2011-0021720).

References

Chandrashekhara, K., Agarwal, A.N., 1993. Active vibration control of laminated composite plates using piezoelectric devices: a finite element approach. J. Intell. Mater. Syst. Struct. 4 (4), 496–508.
Chattopadhyay, A., Seeley, C.E., 1997. A higher order theory for modeling composite laminates with induced strain actuators. Composites Part B 28 (3), 243–252.
Cho, M., Kim, H.S., 2000. Iterative free-edge stress analysis of composite laminates under extension, bending, twisting and thermal loadings. Int. J. Solids Struct. 37 (3), 435–459.
Chopra, I., 2002. Review of state of art of smart structures and integrated systems. AIAA J. 40 (11), 2145–2187.
Detwiler, D.T., Shen, M.H., Venkayya, V.B., 1995. Finite element analysis of laminated composite structures containing distributed piezoelectric actuators and sensors. Finite Elem. Anal. Des. 20 (2), 87–100.
Flanagan, G., 1994. An efficient stress function approximation for the free-edge stresses in laminates. Int. J. Solids Struct. 31 (7), 941–952.
Ghugal, Y.M., Shimpi, R.P., 2002. A review of refined shear deformation theories of isotropic and anisotropic laminated plates. J. Reinf. Plast. Compos. 21 (9), 775–813.
Herakovich, C.T., 2012. Mechanics of composites: a historical review. Mech. Res. Commun. 41, 1–20.
Izadi, M., Tahani, M., 2010. Analysis of interlaminar stresses in general cross-ply laminates with distributed piezoelectric actuators. Compos. Struct. 92 (3), 757–768.
Kabir, H.R.H., 1996. A novel approach to the solution of shear flexible rectangular plates with arbitrary laminations. Composites Part B 27 (1), 95–104.
Kapuria, S., Kumari, P., 2013. Extended Kantorovich method for coupled piezoelasticity solution of piezolaminated plates showing edge effects. Proc. R. Soc. A Math. Phys. Eng. Sci. 469 (2151).
Kapuria, S., Kumari, P., Nath, J.K., 2010. Efficient modeling of smart piezoelectric composite laminates: a review. Acta Mech. 214 (1–2), 31–48.
Kassapoglou, C., Lagace, P.A., 1986. An efficient method for the calculation of interlaminar stresses in composite materials. J. Appl. Mech. 53 (4), 744–750.
Kim, H.S., Cho, M., Kim, G.I., 2000b. Free-edge strength analysis in composite laminates by the extended Kantorovich method. Compos. Struct. 49 (2), 229–235.
Kim, H.S., Zhou, X., Chattopadhyay, A., 2002b. Interlaminar stress analysis of shell structures with piezoelectric patch including thermal loading. AIAA J. 40 (12), 2517–2525.
Kim, H.S., Chattopadhyay, A., Nam, C., 2002a. Implementation of a coupled thermo-piezoelectric-mechanical model in the LQG controller design for smart composite shells. J. Intell. Mater. Syst. Struct. 13 (11), 713–724.
Kim, H.S., Ghoshal, A., Kim, J., Choi, S.B., 2006. Transient analysis of delaminated smart composite structures by incorporating the Fermi–Dirac distribution function. Smart Mater. Struct. 15 (2), 221.
Kim, H.S., Rhee, S.Y., Cho, M., 2008. Simple and efficient interlaminar stress analysis of composite laminates with internal ply-drop. Compos. Struct. 84 (1), 73–86.
Kim, H.S., Cho, M., Lee, J., Deheeger, A., Grédiac, M., Mathias, J.D., 2010. Three dimensional stress analysis of a composite patch using stress functions. Int. J. Mech. Sci. 52 (12), 1646–1659.
Kim, H.S., Kim, J.H., Kim, J., 2011. A review of piezoelectric energy harvesting based on vibration. Int. J. Precis. Eng. Manuf. 12 (6), 1129–1141.
Konieczny, S., Woźniak, C., 1994. Corrected 2D-theories for composite plates. Acta Mech. 103 (1–4), 145–155.
Lee, C.K., 1990. Theory of laminated piezoelectric plates for the design of distributed sensors/actuators: part I: governing equations and reciprocal relationship. J. Acoust. Soc. Am. 87 (3), 1144–1158.
Lee, J., Cho, M., Kim, H.S., 2011. Bending analysis of a laminated composite patch considering the free-edge effect using a stress-based equivalent single-layer composite model. Int. J. Mech. Sci. 53 (8), 606–616.
Lekhnitskii, S.G., 1963. Theory of Elasticity of an Anisotropic Body. Holden-Day, San Francisco.
Pipes, R.B., Pagano, N.J., 1970. Interlaminar stresses in composite laminates under uniform axial extension. J. Compos. Mater. 4 (4), 538–548.
Reddy, J.N., 1999. On laminated composite plates with integrated sensors and actuators. Eng. Struct. 21 (7), 568–593.
Rhee, S.Y., Cho, M., Kim, H.S., 2006. Layup optimization with GA for tapered laminates with internal plydrops. Int. J. Solids Struct. 43 (16), 4757–4776.
Robbins, D.H., Reddy, J.N., 1993. Modelling of thick composites using a layerwise laminate theory. Int. J. Numer. Methods Eng. 36 (4), 655–677.
Spilker, R.L., Chou, S.C., 1980. Edge effects in symmetric composite laminates: importance of satisfying the traction-free-edge condition. J. Compos. Mater. 14, 2–20.
Tahani, M., Nosier, A., 2003. Three-dimensional interlaminar stress analysis at free edges of general cross-ply composite laminates. Mater. Des. 24 (2), 121–130.
Wang, S.S., Choi, I., 1982a. Boundary-layer effects in composite laminates: part 1—free-edge stress singularities. J. Appl. Mech. 49 (3), 541–548.
Wang, S.S., Choi, I., 1982b. Boundary-layer effects in composite laminates: part 2—free-edge stress solutions and basic characteristics. J. Appl. Mech. 49 (3), 549–560.
Wang, Y.Y., Lam, K.Y., Liu, G.R., Reddy, J.N., Tani, J., 1997. A strip element method for bending analysis of orthotropic plates. JSME Int. J. 40 (4), 398–406.
Yin, W.L., 1994a. Free-edge effects in anisotropic laminates under extension, bending and twisting, part I: a stress-function-based variational approach. J. Appl. Mech. 61 (2), 410–415.
Yin, W.L., 1994b. Free-edge effects in anisotropic laminates under extension, bending, and twisting, part II: eigenfunction analysis and the results for symmetric laminates. J. Appl. Mech. 61 (2), 416–421.
Zhu, C., Lam, Y.C., 1998. A Rayleigh-Ritz solution for local stresses in composite laminates. Compos. Sci. Technol. 58 (3–4), 447–461.